Sonoelectrochemical synthesis of highly photoelectrochemically active TiO_2 nanotubes by incorporating CdS nanoparticles

2009 Nanotechnology 20 295601

(http://iopscience.iop.org/0957-4484/20/29/295601)

Nanotechnology **20** (2009) 295601 (6pp) doi:10.1088/0957-4484/20/29/295601

Sonoelectrochemical synthesis of highly photoelectrochemically active TiO_2 nanotubes by incorporating CdS nanoparticles

ChengLin Wang[1], Lan Sun[1], Hong Yun[1], Jing Li[1], YueKun Lai[1] and ChangJian Lin[1,2]

[1] Department of Chemistry, College of Chemistry and Chemical Engineering, Xiamen University, Xiamen 361005, People's Republic of China
[2] State Key Laboratory of Physical Chemistry of Solid Surfaces, Xiamen University, Xiamen 361005, People's Republic of China

E-mail: sunlan@xmu.edu.cn and cjlin@xmu.edu.cn

Received 27 March 2009, in final form 5 May 2009
Published 1 July 2009
Online at stacks.iop.org/Nano/20/295601

Abstract

Self-organized anodic TiO_2 nanotube arrays (TiO_2NTs) are functionalized with CdS nanoparticle based perfusion and deposition through a single-step sonoelectrodeposition method. Even controlled at 50 °C, CdS nanoparticles with smaller size and more homogeneous distribution are successfully synthesized in dimethyl sulfoxide (DMSO) under ultrasonic irradiation. Moreover, TiO_2 nanotubes can be filled with nanoparticles because of the ultrasonic effect. The CdS incorporated TiO_2NTs (CdS–TiO_2NTs) effectively harvest solar light in the UV as well as the visible light (up to 480 nm) region. Compared with pure TiO_2NTs, a more than ninefold enhancement in photocurrent response is observed using the CdS–TiO_2NTs. Maximum incident photon to charge carrier efficiency (IPCE) values of 99.95% and 9.85% are observed respectively for CdS–TiO_2 nanotubes and pure TiO_2NTs. The high value of IPCE observed with the CdS–TiO_2NTs is attributed to the increased efficiency of charge separation and transport of electrons. A schematic diagram is proposed to illustrate the possible process of CdS formation in nanotubes under sonochemical and electrochemical conditions.

(Some figures in this article are in colour only in the electronic version)

1. Introduction

Highly ordered titania (TiO_2) nanotube arrays (TiO_2NTs) synthesized by anodic oxidation of titanium (Ti) are of great interest because of various attractive applications based on solar light conversion [1, 2]. However, as is well known, the wide band gap of TiO_2 (3.2 eV) limits the absorption of sunlight to the ultraviolet region of the solar spectrum. Cadmium sulfide (CdS) is one of the most important II–VI semiconductors used in various photoelectronic devices [3]. Coupling TiO_2NTs electrodes with the CdS semiconductor seems to be a promising approach to enhance their photoresponse in the UV region as well as visible light [4–7]. Previous methods of CdS preparation usually require high vacuum and/or high temperatures, which is necessary to produce gaseous precursor molecules or atoms to realize effective CdS synthesis [8–13]. Moskovits *et al* have developed an electrochemical fabrication of CdS nanowires or nanotube arrays in dimethyl sulfoxide (DMSO) by direct current (DC) electrodeposition [14]. CdS prepared in organic solvent has more uniform crystal phases and higher purity than that in aqueous solution [14–17]. Although this method offers a simple and controllable way of synthesizing CdS nanomaterials, reaction temperatures of 110 °C are typically required to dissolve elemental sulfur in DMSO. High temperatures may result in the conglomeration of CdS nanoparticles, which lowers the photoresponse to sunlight. Furthermore, the air or dissolved gas in nanotubes blocks the

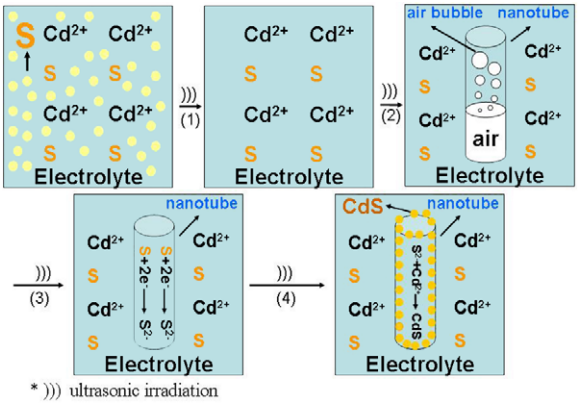

Scheme 1. A schematic diagram of the possible sonoelectrochemical deposition interaction.

formation of CdS nanoparticles in nanotubes [18]. Therefore, CdS is usually piled on the orifice of TiO_2 nanotubes, which causes a decrease of the photoactivity.

In recent decades, the use of ultrasound technology in chemistry has developed rapidly, and combining sonochemistry with electrochemistry has been proven to be efficient in the preparation of various nanomaterials [19–26]. Ultrasound gives rise to high energy via the process of acoustic cavitations, making sonochemistry a unique interaction of energy and matters. Therefore, we reason that the formation of CdS nanoparticles may be allowed by the short energy bursts of ultrasound at lower environmental temperatures in DMSO. TiO_2 nanotubes are probably filled with CdS nanoparticles due to expelling air from the nanotubes under ultrasonic irradiation. A schematic diagram of the process in this work is depicted in scheme 1. The deposition processes would be composed of four steps. (1) Dissolution of elemental sulfur: the effect of ultrasound in a liquid medium is primarily caused by cavitations [27], which promotes the dissolution of elemental sulfur via local high temperature of ultrasound. (2) Expelling air from the nanotube: the air in the nanotube hinders the electrolyte inpouring after the TiO_2 nanotube electrode is immersed in the electrolyte. In a push–pull regime, bubbles are formed from the dissolved gas and air in the nanotube. Then the bigger bubbles can be effectively expelled from the electrolyte by oscillation of the entire system. (3) Reduction of element sulfur to S^{2-} on the TiO_2 nanotube. (4) Formation of CdS nanoparticles in the TiO_2 nanotube.

In this work, even at 50 °C, CdS nanoparticles have been successfully synthesized and placed into self-organized TiO_2NTs electrodes by the sonoelectrochemical technique in DMSO. A detailed synthesis process, characterization, and photoactivity of this CdS–TiO_2NTs catalyst are discussed.

2. Experimental details

Highly ordered TiO_2NTs are prepared by electrochemical anodic oxidation. Prior to electrochemical anodization, Ti samples (1 × 1 cm^2) are mechanically ground with emery papers, then degreased in an ultrasonic bath in acetone, anhydrous ethanol, and deionized (DI) water, successively, followed by rinsing with DI water and drying in air. The electrochemical anodization is carried out in a two-electrode electrochemical cell connected to a DC power supply. A Pt foil acts as a counter-electrode. Ti samples are immersed in a 0.5 wt% HF electrolyte and subjected to a constant 20 V anodic potential for 20 min at room temperature (∼25 °C). The anodized samples are rinsed with DI water and dried in air. Subsequently, TiO_2NTs are annealed at 450 °C in ambient air for 2 h with heating and cooling rates of 5 °C min^{-1} to induce anatase crystallization [28].

The CdS–TiO_2NTs are prepared by the sonoelectrochemical deposition method using a two-electrode system comprising a TiO_2NTs working electrode (1 × 1 cm^2) and a Pt foil counter-electrode. A mixed solution of 0.01 M $CdCl_2$ in DMSO with saturated elemental sulfur is used as the electrolyte [16]. Prior to the sonoelectrodeposition, three processes are performed to completely dissolve elemental sulfur. First, the mixed solution was bubbled with flowing N_2 for 30 min in order to remove O_2 and any moisture within the solution [3]. Second, the solution was persistently stirred for 2 h for an even mixing. Third, the mixed solution is irradiated using an ultrasonic generator (KQ2200DB, Kunshan Ultrasonic Instrument Co., Ltd) with a frequency of 40 kHz and ultrasonic intensity of 2.4 kW m^{-2} for 2 h. The temperature was maintained at 50 °C. Then CdS is cathodically electrodeposited at the optimum constant DC density of 0.5 mA cm^{-2} and the ultrasonic intensity of 2.4 kW m^{-2}. Subsequently, the samples were immediately removed from the electrolyte and sequentially rinsed with hot DMSO, acetone and double-distilled water, and finally dried in air at room temperature.

For reference, CdS–TiO_2NTs are prepared by plain DC electrochemical deposition under the same conditions as the sonoelectrochemical deposition, except for the temperature of 110 °C. The CdS nanoparticles can also be sonoelectrodeposited on metallic Ti for 10 min under the same conditions.

The morphologies of the samples are observed by a field emission scanning electron microscope (SEM, LEO-1530) and transmission electron microscopy (TEM, Tecnai-F30). The crystalline structure of the samples is identified by x-ray diffraction (XRD, Philips, Panalytical X'pert, Cu KR radiation). The elemental composition of the nanotube array films is analyzed by x-ray photoelectron spectroscopy (XPS, VG, Physical Electrons Quantum 2000 Scanning Esca Microprob, Al Kα radiation) combined with 4 keV Ar^+ depth profiling. Photoelectrochemical measurements are carried out in 0.1 M Na_2SO_4 using an LHX 150 Xe lamp, a SBP 300 grating spectrometer, and an electrochemical cell with a quartz window. The wavelength-dependent spectral response is measured in a three-electrode configuration with a platinum wire counter-electrode and a reference saturated calomel electrode (SCE) at zero bias (VS SCE) in the range of 250–500 nm. The photoabsorption properties are recorded with a diffuse reflectance UV–visible spectrometer (DRS) (Varian, Cary 5000).

3. Results and discussion

Figure 1 shows the SEM images of TiO_2NTs before and after CdS sonoelectrodeposition. Figure 1(a) shows that uniform

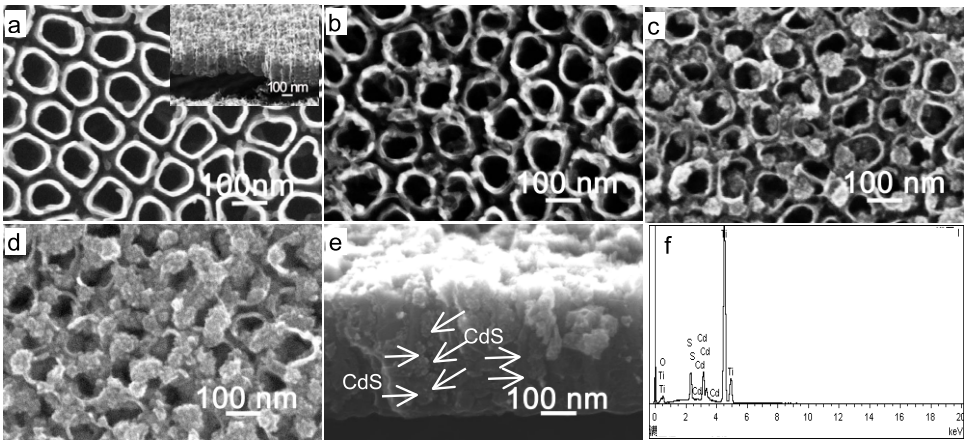

Figure 1. SEM images of TiO_2NTs electrode (a), CdS–TiO_2NTs after CdS sonoelectrochemical deposition at 0.5 mA cm^{-2} for 2 min (b), 5 min (c), 10 min ((d), (e)), respectively. (f) EDS spectrum of CdS–TiO_2NTs sample.

TiO_2 nanotubes are formed with a tube size of about 100 nm in diameter, with a wall thickness of 15 nm and a length of 400 nm (shown in the inset of figure 1(a)). Figures 1(b) and (c) are SEM images of the prepared CdS–TiO_2NTs after CdS sonoelectrodeposition at 0.5 mA cm^{-2} for 2 min and 5 min, respectively. It can be seen that just a few CdS nanoparticles are deposited upon TiO_2NTs. Figure 1(d) is a SEM image of CdS–TiO_2NTs after CdS sonoelectrodeposition for 10 min. It is clearly indicated that TiO_2NTs are extensively covered with a relatively uniform layer of CdS nanoparticle 'groups'. It is noteworthy that the corresponding cross-sectional SEM image (figure 1(e)) shows that the nanotubes are fully filled with CdS nanoparticles (marked with arrows).

The mentioned observations confirm well our reasoning in scheme 1. The above SEM images also reveal that the sonoelectrochemical deposition process does not damage the ordered structure of the TiO_2NTs. The composition of the nanoparticles is determined by an energy dispersive x-ray spectroscopy (EDS) experiment. The corresponding EDS spectrum in figure 1(f) shows the presence of Ti, O, Cd and S.

The CdS–TiO_2NTs are further investigated by using a transmission electron microscope (TEM) (see figure 2). It is clearly indicated that the sample has an ordered tubular structure (marked with white arrows), and the CdS nanoparticles (marked with black arrows) have been deposited into the channels of the TiO_2 nanotubes. The composition of the nanoparticles is determined by an energy dispersive x-ray spectroscopy (EDX) experiment, which is carried out in the TEM. The inset of figure 2 shows a typical EDX spectrum. In this spectrum, peaks associated with Ti, O, C, Cu, S and Cd are observed. Ti and O peaks result from TiO_2NTs, while peaks associated with C and Cu result from the copper grid and supporting C film used in TEM experiments. On the other hand, Cd and S peaks result from CdS nanoparticles.

In comparison with the sonoelectrodeposition, a SEM image of the CdS–TiO_2NTs prepared by plain electrodeposition for 5 min is shown in figure 3(a). In contrast with CdS–TiO_2NTs prepared by the sonoelectrodeposition for 5 min (figure 1(c)), the CdS 'cluster' size prepared by the plain electrodeposition is bigger. As shown in figure 3(b), the average diameters of CdS nanoparticles deposited for 5 min respectively by sonoelectrodeposition and plain electrodeposition were about 28.1 and 90.2 nm. Furthermore, the size distribution of CdS nanoparticles deposited by sonoelectrodeposition is more uniform than that by plain electrodeposition.

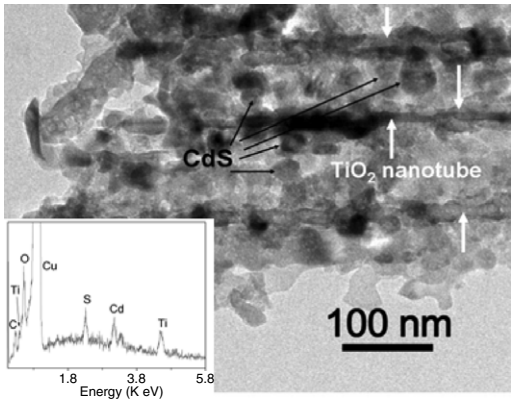

Figure 2. A TEM image of CdS–TiO_2NTs after CdS sonoelectrochemical deposition. (The inset is the corresponding EDX spectrum.)

The structures of the samples are also characterized by XRD. Figure 4 shows a comparison of XRD patterns of TiO_2NTs and CdS–TiO_2NTs. It is apparent that the as-anodized TiO_2NTs only exhibit an amorphous structure (curve (a)), while all annealed samples show clearly the crystalline phase of anatase (curves (b)–(d)) (JCPDS, No. 21-1272). The characteristic peaks corresponding to (002), (101), (102) and (110) crystal planes of CdS are detected from CdS–TiO_2NTs samples (curves (c) and (d)). These peaks can be indexed to a pure CdS hexagonal structure (JCPDS, No. 02-0549) [14]. The broad peaks associated with the hexagonal CdS phase suggest that the size of the CdS nanoparticles is very small.

Figures 5(a) and (b) are, respectively, Cd 3d and S 2p core level XPS scans at higher resolution. The Cd 3d core level XPS spectrum has two peaks at 404.9 eV ($3d_{5/2}$) and 411.7 eV ($3d_{3/2}$), in agreement with reported values for CdS [4, 29]. The

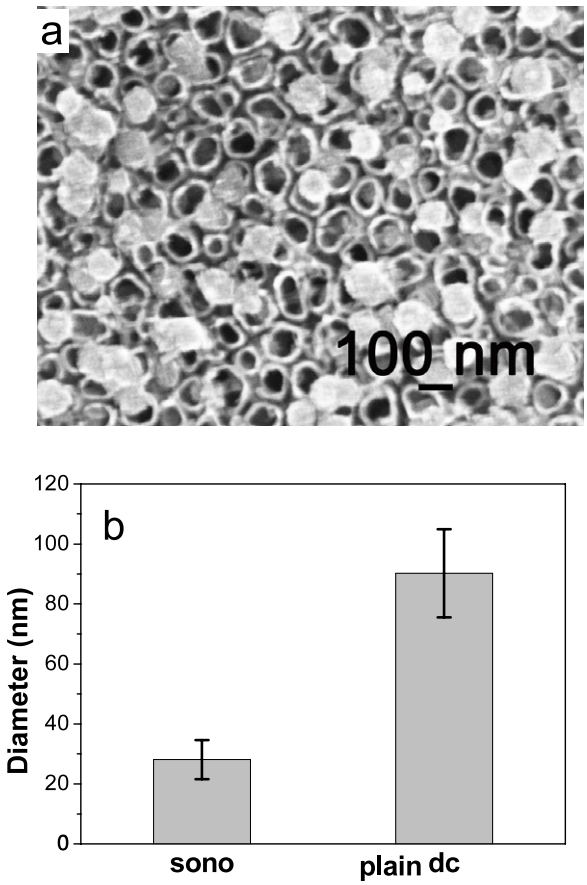

Figure 3. (a) SEM images of CdS–TiO_2NTs after CdS electrochemical deposition at 0.5 mA cm^{-2} for 5 min. (b) The diameter distribution of CdS nanoparticles synthesized by different deposition methods.

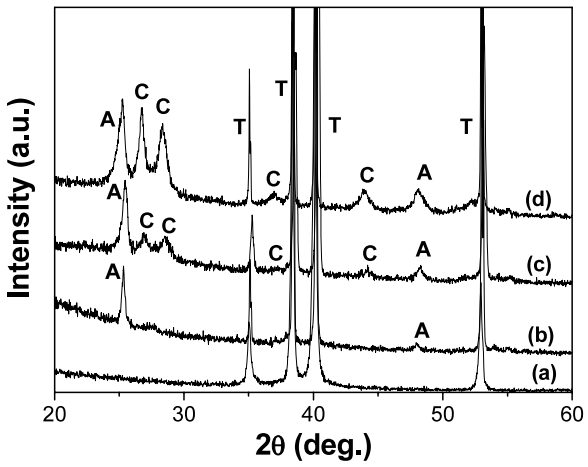

Figure 4. XRD patterns of the as-anodized TiO_2NTs (a), annealed TiO_2NTs at 450 °C (b), and CdS–TiO_2NTs after CdS sonoelectrodeposition for 5 min (c) and 10 min (d), respectively. (A—anatase, C—CdS, T—titanium.)

S 2p core level spectrum indicates that there are two chemically distinct species in the spectrum. The peak at 161.1 eV is for sulfide, in agreement with reported values of the S 2p signal for CdS [4, 29]. Thus CdS is identified both from the sulfide

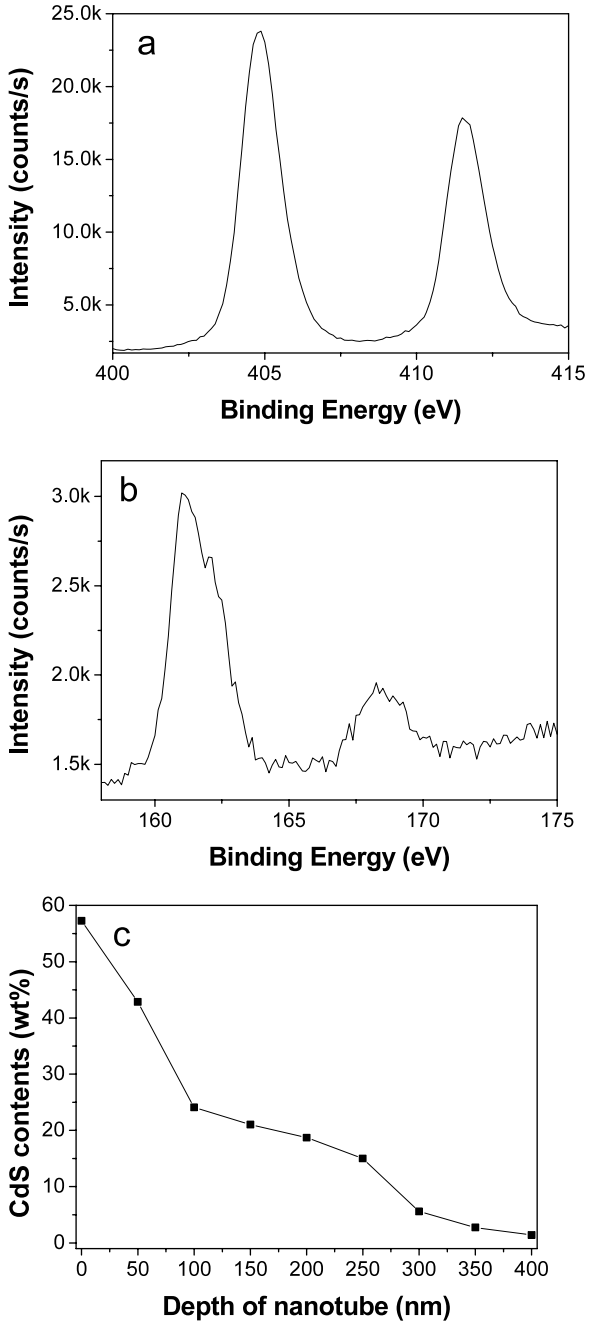

Figure 5. (a) Cd 3d XPS core level spectrum, (b) S 2p XPS core level spectrum, and (c) XPS depth profile of CdS–TiO_2NTs.

peak at 161.1 eV, and also from the peak at 411.7 eV of the Cd $3d_{3/2}$ and 404.9 eV of the Cd $3d_{5/2}$. The CdS amounts residing in CdS–TiO_2NTs are examined by the XPS depth profile of CdS [30, 31]. Figure 5(c) shows the CdS amount as a function of the depth of TiO_2 nanotube. The results prove that CdS nanoparticles are filled inside TiO_2 nanotubes and the deposited CdS amount is inhomogeneous. The maximum CdS amount is at the top of nanotube, then decreases with increasing depth of the TiO_2 nanotube. CdS nanoparticles are mainly perfused into nanotubes between 0 and 250 nm in depth.

The UV–vis DRS of TiO_2NTs and CdS–TiO_2NTs samples is given in figure 6. The pure TiO_2NTs exhibit a fundamental

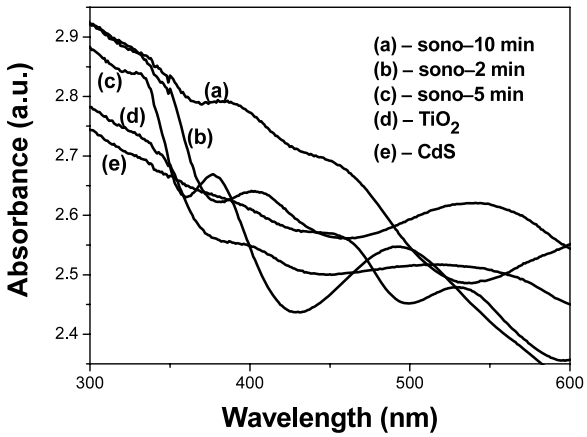

Figure 6. The UV–vis DRS of TiO_2NTs and CdS–TiO_2NTs samples.

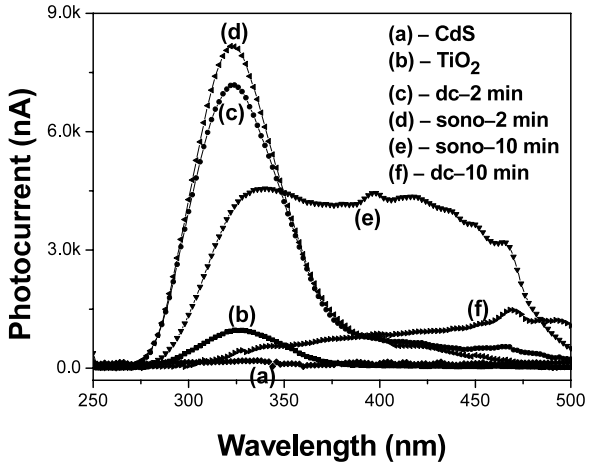

Figure 7. Photocurrent spectra of TiO_2NTs, CdS layer and various CdS–TiO_2NTs electrodes.

absorption edge corresponding to the band-gap energy of 3.2 eV in the ultraviolet region. Comparatively, CdS–TiO_2NTs samples show enhanced absorptions in the range from 350 to 480 nm with increasing sonoelectrodeposition time. When CdS is deposited respectively for 2 and 5 min, the absorption edges of CdS–TiO_2NTs samples show a slight blue-shift, which may be attributed to the small size of the CdS nanoparticles.

The absorption edge of CdS-TiO_2NTs after CdS deposition for 10 min shows an obvious red-shift and the corresponding wavelength is extended to 480 nm [32].

A comparison of the photocurrent spectra of the pure TiO_2NTs electrode, the Ti electrode covered by a CdS layer and the CdS–TiO_2NTs electrodes is presented in figure 7. It is apparent that the photocurrent of CdS–TiO_2NTs electrodes is higher than those of either TiO_2NTs or the CdS layer at all the wavelengths. Furthermore, the CdS–TiO_2NTs electrodes prepared using the sonoelectrodeposition have a stronger photocurrent and a broader photoresponse than the CdS–TiO_2NTs electrodes prepared using the electrodeposition under the same deposition conditions. For the CdS–TiO_2NTs electrode prepared using sonoelectrodeposition for 10 min, not only is the photocurrent much stronger than that of either TiO_2NTs or the CdS–TiO_2NTs electrode prepared using plain electrodeposition, but also the photocurrent response range increases in the range from 280 to 475 nm. Considering the analysis in figure 6, the results prove that the CdS–TiO_2NTs are able to harvest solar light much more effectively than TiO_2NTs under visible light illumination due to the adequate filling of CdS inside TiO_2NTs and a uniform distribution of CdS on/in TiO_2NTs.

The incident photon to charge carrier generation efficiency (IPCE) at different wavelengths is determined from the short circuit photocurrents (I_{sc}) monitored at different excitation wavelengths (λ) to compare the photoresponse of the samples using an equation [33]

$$\mathrm{IPCE}(\%) = [1240 \times I_{sc}(\mathrm{mA\ cm^{-2}})]/[\lambda(\mathrm{nm}) \times I_{inc}(\mathrm{W\ cm^{-2}})] \times 100 \quad (1)$$

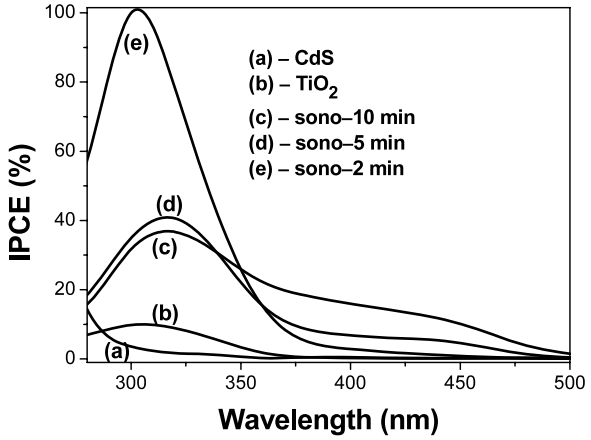

Figure 8. IPCE results of TiO_2NTs, CdS layer and CdS–TiO_2NTs photoelectrodes after sonoelectrodeposition.

where I_{inc} is the incident light power. The IPCE as a function of the excitation wavelength for TiO_2NTs, CdS layer and CdS–TiO_2NTs calculated from the data of figure 7 is shown in figure 8.

A maximum IPCE of 99.95% is achieved for the CdS–TiO_2NTs electrode prepared by sonoelectrodeposition for 2 min at the wavelength of 300 nm. However, under the same conditions, the IPCE values of 9.82% for TiO_2NTs and 3.58% for CdS layer are observed. Lower IPCE values indicate that a larger fraction of carriers is lost to charge recombination. Moreover, for the CdS–TiO_2NTs electrode prepared by sonoelectrodeposition for 10 min, the quantum efficiencies are significantly enhanced at wavelengths from 280 to 475 nm, which suggests electrons (e^-) and holes (h^+) can be separated more effectively. The strong photoresponse may be attributed to three major improvements. Firstly, during the ultrasonic process, TiO_2 nanotubes are filled with a host of CdS nanoparticles with smaller diameter, and uniform size distribution is obtained. Secondly, increased light absorbability and better light scattering are produced within the CdS–TiO_2 nanocomposite structure. Additionally, the photo-generated

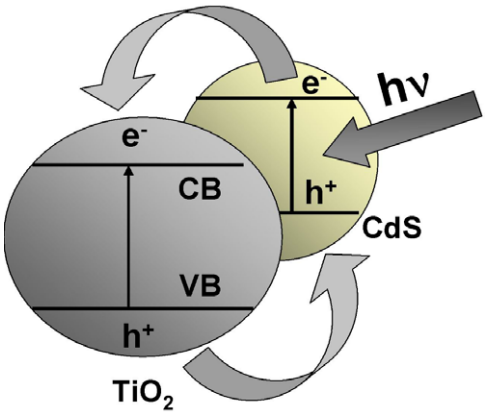

Figure 9. The main charge-transfer process between TiO_2 and CdS after being excited by light. (CB and VB refer to the energy levels of the conduction and valence bands, respectively, for the CdS nanoparticle and TiO_2 nanotube.)

charge carriers in the CdS–TiO_2 nanotubular structure are separated more efficiently than in the pure TiO_2 nanotube structure due to the favorable electron (e^-) and hole (h^+) transfer. Figure 9 illustrates the main charge-transfer processes between TiO_2 and CdS after being activated by the light. Since the conduction band of bulk CdS is ca. 0.5 V, more negative than that of TiO_2 [4], the coupling of the semiconductors has a beneficial role in improving charge separation. Excited electrons from the CdS nanoparticle can quickly transfer to the TiO_2 nanotube, arriving at the photocurrent collector (Ti substrate) through the highly ordered TiO_2 nanotube array structure. The responsive photocurrent intensity is usually able to directly represent the overall photoelectron-conversion process.

4. Conclusions

In conclusion, we have demonstrated a simple and feasible way, the sonoelectrochemical technique, to successfully synthesize CdS–TiO_2NTs in DMSO at a lower temperature (even at 50 °C). The TiO_2 nanotubes can be filled with CdS nanoparticles by using an ultrasonic technique. Compared with the CdS–TiO_2NTs prepared by the plain electrodeposition, the CdS–TiO_2NTs prepared by the sonoelectrodeposition display an enhanced photocurrent and the photocurrent response is extended to 480 nm. In the coupled semiconductor system, the small band-gap semiconductor CdS acts as a photosensitizer for the TiO_2. Through transfer of the photoexcited electron from the CdS nanoparticle to the TiO_2 nanotube, an enhanced photocatalytic reaction can occur. The application of the sonoelectrochemical technique leads to better solar light harvest in the visible light region. Thus, the sonoelectrochemical method will provide a promising technique to fabricate excellent composite materials at lower temperature in organic solvent.

Acknowledgments

Financial support for this study has been provided by the Natural Science Foundation of China and Fujian Province (20773100, U0750015), Technical Program of Fujian Province and Xiamen City, China (2007H0031, 3502Z20073004).

References

[1] Mor G K, Varghese O K, Paulose M, Shankar K and Grimes C A 2006 *Sol. Energy Mater. Sol. Cells* **90** 2011
[2] Macak J M, Tsuchiya H, Ghicov A, Yasuda K, Hahn R, Bauer S and Schmuki P 2007 *Curr. Opin. Solid State Mater. Sci.* **11** 3
[3] Tada H, Mitsui T, Kiyonaga T, Akita T and Tanaka K 2006 *Nat. Mater.* **5** 782
[4] Chen S, Paulose M, Ruan C, Mor G K, Varghese O K, Kouzoudis D and Grimes C A 2006 *J. Photochem. Photobiol.* A **177** 177
[5] Yin Y X, Jin Z G and Hou F 2007 *Nanotechnology* **18** 495608
[6] Xiao M W, Wang L S, Wu Y D, Huang X J and Dang Z 2008 *Nanotechnology* **19** 015706
[7] Sun W T, Yu Y, Pan H Y, Gao X F, Chen Q and Peng L M 2008 *J. Am. Chem. Soc.* **130** 1124
[8] Fujii M, Kawai T and Kawai S 1988 *Sol. Energy Mater.* **18** 23
[9] O'Brien P, Walsh J R, Watson I M, Hart L and Silva S R P 1996 *J. Cryst. Growth* **167** 133
[10] Cheon J and Zink J I 1997 *J. Am. Chem. Soc.* **119** 3838
[11] Fujita S, Kawakami Y and Fujita S 1996 *J. Cryst. Growth* **164** 196
[12] Fraser D B and Melchior H 1972 *J. Appl. Phys.* **43** 3120
[13] Meng L and Santos M P 1995 *Vacuum* **46** 1001
[14] Routkevitch D, Bigioni T, Moskovits M and Xu J M 1996 *J. Phys. Chem.* **100** 14037
[15] Yamaguchi K, Yoshida T, Sugiura T and Minoura H 1998 *J. Phys. Chem.* B **102** 9677
[16] Xu D S, Xu Y J, Chen D P, Guo G L, Gui L L and Tang Y Q 2000 *Chem. Phys. Lett.* **325** 340
[17] Peng T Y, Yang H P, Dai K, Pu X L and Hirao K 2003 *Chem. Phys. Lett.* **379** 432
[18] Banerjee S, Mohapatra S K, Das P P and Misra M 2008 *Chem. Mater.* **20** 6784
[19] Mastai Y, Hodes G, Polsky R, Koltypin Y and Gedanken A 1999 *J. Am. Chem. Soc.* **121** 10047
[20] Zhu J, Liu S, Palchik O, Koltypin Y and Gedanken A 2000 *Langmuir* **16** 6396
[21] Mastai Y, Homyonfer M, Gedanken A and Hodes G 1999 *Adv. Mater.* **11** 1010
[22] Delplancke J L, Dille J, Reisse J, Long G J, Mohan A and Grandjean F 2000 *Chem. Mater.* **12** 946
[23] Zhu J, Aruna S T, Koltypin Y and Gedanken A 2000 *Chem. Mater.* **12** 143
[24] Durant A, Francois H, Reisse J and Kirsch-Demesmaeker A 1996 *Electrochim. Acta* **41** 277
[25] Zhu J J, Qiu Q F, Wang H, Zhang J R, Zhu J M and Chen Z Q 2002 *Inorg. Chem. Commun.* **5** 242
[26] Cornpton R G, Eklund J C and Marken F 1997 *Electroanalysis* **9** 509
[27] Gaplovsky A, Gaplovsky M, Kimura T, Toma S, Donovalova J and Vencel T 2007 *Ultrason. Sonochem.* **14** 695
[28] Gong D, Grimes C A, Varghese O K, Hu W, Singh R S, Chen Z and Dickey E C 2001 *J. Mater. Res.* **16** 3331
[29] Kundu M, Khosravi A A and Kulkarni S K 1997 *J. Mater. Sci.* **32** 245
[30] Karthik S, Kong C T, Mor G K and Grimes C A 2006 *J. Phys. D: Appl. Phys.* **39** 2361
[31] Ristova M and Ristov M 2001 *Appl. Surf. Sci.* **181** 68
[32] Kokai J and Rakhshani A E 2004 *J. Phys. D: Appl. Phys.* **37** 1970
[33] Robel I, Subramanian V, Kuno M and Kamat P V 2006 *J. Am. Chem. Soc.* **128** 2385